Journal of Visualized Experiments

Visualizing uniaxial-strain-manipulation of antiferromagnetic domains in Fe1+yTe using spin-polarized scanning tunneling microscope

--Manuscript Draft--

Article Type:	Invited Methods Article - JoVE Produced Video
Manuscript Number:	JoVE59203R2
Full Title:	Visualizing uniaxial-strain-manipulation of antiferromagnetic domains in Fe1+yTe using spin-polarized scanning tunneling microscope
Keywords:	Uniaxial strain, scanning tunneling microscopy, spin-polarized STM, iron-based superconductors; antiferromagnetic domains, unconventional superconductivity
Corresponding Author:	Pegor Aynajian UNITED STATES
Corresponding Author's Institution:	
Corresponding Author E-Mail:	paynajia@binghamton.edu
Order of Authors:	Pegor Aynajian
	Mariam Kavai
	Ioannis Giannakis
	Justin Leshen
	Joel Friedman
	Pawel Zajdel
Additional Information:	
Question	**Response**
Please indicate whether this article will be Standard Access or Open Access.	Standard Access (US$2,400)
Please indicate the **city, state/province, and country** where this article will be **filmed**. Please do not use abbreviations.	Vestal, NY, USA

Binghamton University
The State University of New York

Department of Physics, Applied Physics and Astronomy
Smart Energy Building
4400 Vestal Parkway East
Binghamton, NY 13902
Phone: (607) 777 4627
Email: aynajian@binghamton.edu
https://www.binghamton.edu/physics/aynajian-group/

November 14, 2018

Dear Editor,

We are resubmitting the manuscript titled "Visualizing uniaxial-strain-manipulation of antiferromagnetic domains in $Fe_{1+y}Te$ using spin-polarized scanning tunneling microscope" to be considered as a letter in **JoVE**. We have updated the paper following the editorial comments. We have also added new paragraphs describing the comments raised by the referees.

Together with this cover letter we are submitting the new manuscript, updated figures and one-to-one response to all referee comments.

We thank you for your time and consideration.

Sincerely,

Pegor Aynajian

TITLE:

Visualizing Uniaxial-strain Manipulation of Antiferromagnetic Domains in $Fe_{1+Y}Te$ Using a Spin-polarized Scanning Tunneling Microscope

AUTHORS & AFFILIATIONS:

Mariam Kavai[1], Ioannis Giannakis[1], Justin Leshen[1], Joel Friedman[1], Paweł Zajdel[2], Pegor Aynajian[1]

[1]Department of Physics, Applied Physics and Astronomy, Binghamton University, Binghamton, NY, USA

[2]Institute of Physics, University of Silesia, Chorzów, Poland

Corresponding author:

Pegor Aynajian (paynajia@binghamton.edu)

Tel: (607)-777-4627

Email addresses of co-authors:

Mariam Kavai (mkavai1@binghamton.edu)

Ioannis Giannakis (igianna1@binghamton.edu)

Justin Leshen (jleshen1@binghamton.edu)

Joel Friedman (jfried29@binghamton.edu)

Paweł Zajdel (pawel.zajdel@us.edu.pl)

KEYWORDS:

uniaxial strain, scanning tunneling microscopy, spin-polarized STM, iron-based superconductors, antiferromagnetic domains, unconventional superconductivity

SUMMARY:

Using uniaxial strain combined with spin-polarized scanning tunneling microscopy, we visualize and manipulate the antiferromagnetic domain structure of $Fe_{1+y}Te$, the parent compound of iron-based superconductors.

ABSTRACT:

The quest to understand correlated electronic systems has pushed the frontiers of experimental measurements toward the development of new experimental techniques and methodologies. Here we use a novel home-built uniaxial-strain device integrated into our variable temperature scanning tunneling microscope that enables us to controllably manipulate in-plane uniaxial strain in samples and probe their electronic response at the atomic scale. Using scanning tunneling microscopy (STM) with spin-polarization techniques, we visualize antiferromagnetic (AFM) domains and their atomic structure in $Fe_{1+y}Te$ samples, the parent compound of iron-based superconductors, and demonstrate how these domains respond to applied uniaxial strain. We observe the bidirectional AFM domains in the unstrained sample, with an average domain size of ~50–150 nm, to transition into a single unidirectional domain under applied uniaxial strain. The findings presented here open a new direction to utilize a valuable tuning parameter in STM, as well as other spectroscopic techniques, both for tuning the electronic properties as for inducing

symmetry breaking in quantum material systems.

INTRODUCTION:

High-temperature superconductivity in cuprates and iron-based superconductors is an intriguing state of quantum matter[1,2]. A major challenge in understanding superconductivity is the locally intertwined nature of various broken symmetry states, such as electronic nematic and smectic phases (that break rotational and translational symmetries of the electronic states), with superconductivity[3–7]. Manipulation and deliberate tuning of these broken symmetry states is a key objective toward understanding and controlling superconductivity.

Controlled strain, both uniaxial and biaxial, is a well-established technique to tune the collective electronic states in condensed matter systems[8–22]. This clean tuning, without the introduction of disorder through chemical doping, is commonly used in various kinds of experiments to tune bulk electronic properties[23–26]. For example, uniaxial pressure has proved to have an immense effect on superconductivity in Sr_2RuO_4[13] and cuprates[27] and on the structural, magnetic, and nematic phase transitions of iron-based superconductors[10,14,28,29] and was recently demonstrated in tuning the topological states of SmB_6[24]. However, the use of strain in surface-sensitive techniques, such as STM and angle-resolved photoemission spectroscopy (ARPES), has been limited to in situ-grown thin films on mismatched substrates[19,26,30]. The major challenge with applying strain to single crystals in surface-sensitive experiments is the need to cleave the strained samples in ultrahigh vacuum (UHV). In the last few years, an alternative direction has been to epoxy a thin sample on piezo stacks[9,10] or on plates with different coefficients of thermal expansion[19,31]. Yet in both cases, the magnitude of the applied strain is quite limited.

Here we demonstrate the use of a novel mechanical uniaxial-strain device that allows researchers to strain a sample (compressive strain) without constraints and simultaneously visualize its surface structure using STM (see **Figure 1**). As an example, we use single crystals of $Fe_{1+y}Te$, where y = 0.10, the parent compound of the iron chalcogenide superconductors (y is the excess iron concentration). Below T_N = ~60 K, $Fe_{1+y}Te$ transitions from a high-temperature paramagnetic state into a low-temperature antiferromagnetic state with a bicollinear stripe magnetic order[26,32,33] (see **Figure 3A,B**). The magnetic transition is further accompanied by a structural transition from tetragonal to monoclinic[26,34]. The in-plane AFM order forms detwinned domains with the spin structure pointing along the long b-direction of the orthorhombic structure[33]. By visualizing the AFM order with spin-polarized STM, we probe the bidirectional domain structure in unstrained $Fe_{1+y}Te$ samples and observe their transition into a single large domain under applied strain (see the schematic in **Figure 3C-E**). These experiments show the successful surface tuning of the single crystals using the uniaxial-strain device presented here, the cleaving of the sample, and the simultaneous imaging of its surface structure with the scanning tunneling microscope. **Figure 1** shows the schematic drawings and pictures of the mechanical strain device.

PROTOCOL:

NOTE: The U-shaped body is made of 416-grade stainless steel, which is stiff and has a low coefficient of thermal expansion (CTE), ~9.9 µm/(m·°C), as compared to ~17.3 µm/(m·°C) for 304-

grade stainless steel.

1. Mechanical uniaxial-strain device

1.1. Clean the U-shaped device, the micrometer screws (1–72 corresponding to 72 rotations per inch), the Belleville spring disks, and the base plate by sonicating them separately in acetone first and then in isopropanol, for 20 min each, in an ultrasonic bath sonicator. This removes any impurities/particles. This process should be carried out in the hood.

1.2. Bake them in an oven for 15–20 min to get rid of any water residue and to degas.

1.3. Using a sharp razor blade, while observing under an optical microscope, cut the $Fe_{1+y}Te$ sample to size, namely 1 mm x 2 mm x 0.1 mm.

1.4. Assemble the parts together as shown in **Figure 1C**, first panel. The opening inside the U is 1 mm and can be tuned smaller or large by a pair of micrometer screws located on the sides of the device.

2. Application of the strain

2.1. In two separate dishes, mix silver epoxy (H20E) and nonconductive epoxy (H74F) according to the instructions on the epoxy data sheet.

2.2. On the U-shaped device, apply a thin layer of silver epoxy (H20E) to create electrical contact, and mount the sample (of a size of 1 mm x 2 mm x ~0.1 mm) with its long axis oriented along the b-axis of the $Fe_{1+y}Te$ sample, on top of the device, across the 1 mm gap, as shown in **Figure 1C**. In a convection oven, bake the device for 15 min at 120 °C.

2.3. Cover the two sides of the sample with nonconductive epoxy so that the sample is firmly supported on the device. Bake for 20 min at 100 °C.

2.3.1. Using an optical microscope, examine the position of the sample from all angles to check for a parallel alignment of the sides of the sample with the gap.

2.3.2. Optionally, place samples within the gap and enforced by H20E and H74F epoxy (**Figure 1C**).

2.4. Under an optical microscope, apply compressive strain by rotating the micrometer screw while observing the surface of the sample.

NOTE: Here we applied a 50° strain, but this can be modified depending on the amount of strain to be applied to the sample. The pressure is transferred to the sample by a series of Belleville spring disks. There should be no cracks or bending of the sample after the pressure is applied.

2.5. Screw the device onto the base plate as shown in **Figure 1B**.

2.5.1. Apply a thin layer of silver epoxy (H20E) from the base plate onto the U-shaped device to create electrical contact between the sample and the plate. Bake for 15 min at 120 °C. Measure the electrical contact using a multimeter.

2.5.2. Using a thin layer of H74F nonconducting epoxy, glue an aluminum post (the same size as the sample) onto the strained sample, perpendicular to the a-b cleaving plane. Bake the assembled device for 20 min until the epoxy is cured.

3. Transfer of the device to the scanning tunneling microscope head

3.1. Transfer the staining device with the sample and the post through the loading dock of the variable-temperature, ultrahigh vacuum scanning tunneling microscope, to the analysis chamber (see **Figure 2A**).

3.2. Using an arm manipulator, knock off the aluminum post in ultrahigh vacuum at room temperature, to expose a freshly cleaved surface.

3.3. Immediately transfer the device (with the strained sample) in situ with another set of manipulators to the scanning tunneling microscope chamber and to the microscope head (see **Figure 2B**), which has been cooled down to 9 K. Carry out all experiments at 9 K.

3.4. Allow the sample to cool down overnight before carrying out the next steps.

4. Carrying out the STM experiments

4.1. Prepare the Pt-Ir tips prior to each experiment by field emission on a Cu (111) surface that has been treated with several rounds of sputtering and annealing.

4.2. Using the voltage applied to the piezoelectric materials in the microscope by an external controller, move the sample stage to align with the tip, then follow by approaching the sample.

4.3. Once the tip is a few Å away from the sample and the tunneling current is registered on the oscilloscope, take topographs at different setpoint biases and setpoint currents.

NOTE: The scanning tunneling microscope is controlled by manufacturer-provided controller and software. For the operation of the microscope, please refer to the user manual/tutorials (http://www.rhk-tech.com/support/tutorials/).

REPRESENTATIVE RESULTS:

STM topographs were measured in constant current mode with a setpoint bias of -12 meV applied to the sample and a setpoint current of -1.5 nA collected on the tip. Pt-Ir tips were used in all experiments. To achieve spin-polarized STM, the scanning tunneling microscope tip has to

be coated with magnetic atoms, which can be quite challenging. In this case of studying $Fe_{1+y}Te$, the sample itself provides a simple means of achieving this. The excess irons (y in $Fe_{1+y}Te$) are weakly bound on the cleaved surface. Scanning the tip at a low bias and with a high enough current exceeding a few nanoamperes brings the tip in close proximity to these Fe atoms and a few of those atoms can be picked up by the tip[35]. The other method that yields a spin-polarized tip is by the rapid decrease of the sample-tip separation until contact is made (on the location of excess iron concentration) as measured by a saturation current. During the process, the excess irons bond onto the tip. The successful preparation of a spin-polarized tip is revealed by the magnetic contrast in the topography, whose periodicity is twice that of the lattice constant of top tellurium atoms. This additional modulation is the antiferromagnetic order in the sample, as discussed further below.

Figure 4A shows a 10 nm atomic-resolution topographical image on an unstrained $Fe_{1+y}Te$ single crystal with a nonmagnetic scanning tunneling microscope tip. The atomic structure seen corresponds to the Te atoms, which are exposed after cleaving the sample (see **Figure 3A**). The Fourier transform (FT) of the topography shows four sharp peaks at the corners of the image along the a- and b-directions, labeled q_{Te}^{a} and q_{Te}^{b}, that correspond to the atomic Bragg peaks. The central broad peak in the FT corresponds to long-wavelength inhomogeneity, which is not relevant for the current study. **Figure 4C** shows another topograph of the same size as in **Figure 4A**, obtained with a magnetic tip. Unidirectional stripes with a periodicity of twice that of the lattice along the a-axis are observed. The FT of the topograph seen in **Figure 4D** shows, in addition to the Bragg peaks, a new pair of satellite peaks at Q_{AFM1}, corresponding to half the Bragg peak momenta and, therefore, twice the real space wavelength. The new structure corresponds to the AFM stripe order of the Fe atoms just below the surface.

On this unstrained sample, it is not difficult to observe twin domain boundaries where the crystal structure with the long b-axis and the accompanying AFM stripe order rotate 90°. **Figure 4E** shows a 25 nm spin-polarized topograph of an AFM twin domain boundary. The FT of the image now shows two pairs of AFM order (highlighted by green and yellow circles). Each magnetic domain contributes to only one pair of the Q_{AFM} peaks in the FT. To visualize this clearly, we Fourier-filtered each pair of AFM peaks and inversed FT back to real space. The results are shown in **Figure 4G,H** highlighting the two unidirectional stripe domains.

Thus, we studied the domain structure and boundaries on the surface on a large scale. **Figure 5A**, **Figure 6A**, and **Figure 7A** display large-scale topographs on three different unstrained samples spanning a total region of slightly over 0.75 µm x 0.75 µm. Several smaller zoomed-in topographs are also shown to highlight the stripe structure. The topographs are taken with a high spatial resolution (1024 x 1024 pixels per 0.25 μm^2) to allow the Fourier filtering and inverse Fourier transform analysis on the large scale. The corresponding domain structures and boundaries are displayed in **Figure 5B**, **Figure 6C**, and **Figure 7H**. Overall, several alternating stripe domains are observed covering the overall equal areas, as expected for these unstrained samples. It is important to note that on this large scale the surface is overall atomically flat, yet a few different structural irregularities, such as line defects (**Figure 5A**) and atomic steps (**Figure 7A**), can be observed. The stripe domains are not affected by these irregularities.

From here, we moved on to the strained sample. **Figure 8** shows a large-scale topograph, spanning a total region of ~1.75 µm x 0.75 µm, which is more than twice the total area spanned in the unstrained samples shown in **Figure 5**, **Figure 6**, and **Figure 7**. In stark contrast, the FT for each topograph shows only one pair of AFM peaks indicating only a single domain on this strained sample. This can further be visualized by the Fourier-filtered iFT analysis confirming the single stripe domain over the entire area. Once again, the unidirectional stripe order is not to be affected by the different surface irregularities in this strained sample.

FIGURE AND TABLE LEGENDS:

Figure 1: Strain device. (**A**) Schematic of the strain device. The U-shaped device has two micrometer screws for the (1) compression and (2) expansion of the device's gap area. The sample can be confined inside the gap as shown in figure panels **A** and **C** or on top of the gap as shown in figure panels **A** and **B**. A combination of H20E and H74F epoxies are applied to the sample and cured at 100 °C. Once the epoxy on the sample is cured, a post of about the same surface area as that of the sample is epoxied onto the sample's surface using H74F. (**B**) The actual setup of the strain device, with a top view, front view, and a zoom-in of the sample. The device is screwed to a sample holder that slides into the microscope head. A contact is created by using conductive epoxy from the device to the sample plate. The transfer of pressure is enabled using a screw and a series of Belleville spring disks. The last panel of **B** shows the strain device set up, ready to be moved into the UHV analysis chamber. (**C**) An alternative method is to have a sample inside the gap of the strain device. In the two middle panels of **C**, a second unstrained sample is epoxied on the device for reference.

Figure 2: Scanning tunneling microscope setup. (**A**) The scanning tunneling microscope setup. The microscope is placed in an acoustic chamber, which is shielded from radio-frequency (RF) noise. (**B**) The microscope head with a bare sample holder. The Pt/Ir tip is visible. The sample stage can be moved by a set of piezo actuators so that the sample is right above the tip. (**C**) The microscope head is placed inside two radiation shields.

Figure 3: $Fe_{1+y}Te$ crystal structure. (**A**) The crystal structure of FeTe with the top layer showing the tellurium atoms. The red dotted lines outline the three unit cells. (**B**) A real-space schematic illustration of the atomic unit cell (red solid line) and magnetic structure (black solid line) of FeTe. The magnetic wavevector λ_{afm} is twice the atomic distance between Te-Te atoms. The arrows on the Fe atoms indicate the spin orientations. (**C**) Schematic diagram illustrating the AFM twin domains that form when cooling, through the structural transition from tetragonal to monoclinic at ~60 to 70 K, with an equal population of the two domains. (**D**) The response of the detwinning process, when an appreciable amount of strain is applied along the b-axis (black arrows) with one domain enhanced (red) and the other domain diminished (blue). (**E**) A complete detwinned domain, which leaves only one single domain. (**F–H**) The FT of the real space in panels **C–E**. The Q_{AFM1} peaks correspond to the red real-space domains, and the Q_{AFM2} peaks correspond to the blue domains. The lattice Bragg peaks are denoted as black dots at the corners of the image.

Figure 4: Unidirectional modulation from unstrained $Fe_{1+y}Te$. (**A**) A 10 nm x 10 nm topograph of the atomic lattice structure of $Fe_{1+y}Te$ with no magnetic contrast. (**B**) The FT of panel **A**, showing the Bragg peaks at the corners of the images (black circles). (**C**) A 10 nm x 10 nm topograph of the magnetic structure of $Fe_{1+y}Te$, measured using a spin-polarized tip. The unidirectional stripes across the a-axis correspond to peaks appearing at $Q_{AFM1} = q_{Te}^{a}/2$ in the FT, as shown in panel **D**. (**E**) A 25 nm x 25 nm topographical image across a twin domain boundary. (**F**) FT of panel **E**, showing the two sets of peaks Q_{AFM1} and Q_{AFM2}. (**G**) Inverse Fourier transform (iFT) of the Q_{AFM1} peaks from panel **F**. The red color corresponds to the high intensity of the Q_{AFM1} peaks. (**H**) iFT of the Q_{AFM2} peaks from panel **F**. The domain boundary is clearly distinct from the images shown in panels **G** and **H**. The inverse Fourier filtering method has been used in subsequent figures to identify the different domains.

Figure 5: Imaging twin domains in unstrained $Fe_{1+y}Te$. (**A**) A 0.75 µm x 0.25 µm topographical image showing twin boundaries. The data was acquired in three adjacent topographical images, each 0.25 µm x 0.25 µm. (**B**) Using iFT, the domain boundaries are distinctly evident. (**C–E**) Zoom-ins of the images marked with an (X) and a yellow-colored dotted box are shown with highlighted, dotted, colored boxes around the boundaries.

Figure 6: Imaging multiple domains from unstrained $Fe_{1+y}Te$. (**A**) A 0.10 µm x 0.10 µm topographical image of an unstrained $Fe_{1+y}Te$. (**B**) The FT of panel **A**, which shows peaks in both directions, namely Q_{AFM1} and Q_{AFM2}. (**C**) The iFT image of panel **A**, indicating the different domains. (**D** and **E**) Zoom-ins of the highlighted yellow- and orange-dotted boxes in panel **A**.

Figure 7: Imaging twin domains from unstrained $Fe_{1+y}Te$. (**A**) Topographical images spanning an area of 0.75 µm x 0.5 µm. (**B–D**) Line cuts of the topograph taken across the black, purple, and green arrows in panel **A**. (**E–G**) Zoom-in of the areas highlighted in the green, brown, and yellow (X) marks in panel **A**. (**H**) iFT of panel **A**, showing the twin domains. The white-dotted lines are the step edges/boundaries. The domains are unaffected by these structural features.

Figure 8: Imaging detwinned domains in strained $Fe_{1+y}Te$. (**A**) A large 1.750 µm x 0.50 µm topography taken on a strained $Fe_{1+y}Te$ sample. (**B** and **C**) The FT of the two largest (0.50 µm x 0.50 µm) single topographs acquiring on one pair of AFM peaks in one direction. (**D**) The Fourier-filtering and iFT process is applied to the images in panel **A**, which shows only a single domain as expected. The dotted line in panel **D** is a step which does not affect the unidirectional domain. (**E**) A zoom-in of the highlighted region in the yellow (X) showing unidirectional stripes. (**F**) A zoom-in of panel **E**, also showing clearly the unidirectional stripes of the detwinned sample. (**G**) The FT of panel **E**. The AFM peaks appear only in one direction, which agrees with the real-space structure in panel **E**.

DISCUSSION:

All operations required to move the samples into and inside the STM are carried out using sets of arm manipulators. The STM is maintained at low temperatures by liquid nitrogen and liquid helium, and the sample cools down for at least 12 h before being approached. This allows the sample and microscope temperature to reach thermal equilibrium. To isolate electric and

acoustic noise, the STM is placed in an acoustic and radio frequency shielded room. The microscope head is further suspended from springs for optimized instrumental stability. The sample stage can be translated by several millimeters that enable access to different parts of the 1 mm strained samples.

Since uniaxial pressure is the tuning parameter in the experiment described here, it is imperative that the thermal stress generated from cooling down is not transferred directly to the sample. For this, we employ a series of Belleville spring disks. Using the working load of the Belleville spring disks of 67 N, and the deflection at working load of 50 µm, we calculate the spring constant for each disk as $k = 1.3 \times 10^6$ N/m, which yields a total spring constant of $k = 1.625 \times 10^5$ N/m for 4 pairs of springs in series. This ensures the thermal stress on the sample through cooling from room temperature to 4 K to be less than 0.05% for an applied strain of 1% and therefore negligible. In the experiment, we rotate the micrometer screw by 50° which corresponds to Δx = 50 µm. The force applied on the sample through the springs can be calculated to be $F = k\Delta x = 8$ N. The pressure is therefore $p = F/A = 8\ \mathrm{N}/(0.1 \times 10^{-6}\ \mathrm{m}^2) = 0.08$ GPa. For a Young's modulus of 70 Gpa for FeTe[36], the applied uniaxial pressure corresponds to 0.1% strain.

A major challenge in integrating the strain devices with the STM is the application of strain without breaking or introducing cracks in the sample. Test experiments on several samples of Bi-2212, $Sr_3Ru_2O_7$, and $Fe_{1+y}Te$ have shown that, depending on the sample thickness, the samples withstand strains of up to ~0.8%–1.0%, corresponding to ~1 GPa of applied pressure. No indications of cracks on the sample surface are observable below this value as seen visually by an optical microscope. Recent work following the same principles has successfully demonstrated the application of ±1% strain on Sr_2RuO_4 [9].

The success of this technique lies in the careful execution of the correct alignment of the sample across the 1 mm gap and application of the strain on the sample without breaking or bending it. Another important consideration is the cleaving process, which allows the exposure of a clean flat surface. This is a random process and works best for materials that cleave easily. A last consideration is having a sharp tip that yields atomic resolution and can pick up some excess iron atoms to achieve magnetic contrast.

In conclusion, the experiments and analysis described here successfully demonstrate the incorporation of our strain device with STM, providing a new tuning parameter that can be invaluable in the study of competing orders in correlated electron systems. The advantage of the current device is the wide range of positive and negative strain that can be applied to the sample. This demonstration may impact other spectroscopic experiments such as ARPES.

ACKNOWLEDGMENTS:
P.A. acknowledges support from the U.S. National Science Foundation (NSF) CAREER under award No. DMR-1654482. Material synthesis was carried out with the support of the Polish National Science Centre grant No 2011/01/B/ST3/00425.

DISCLOSURES:

The authors have nothing to disclose.

REFERENCES:

1. Paglione, J., Greene, R. L. High-temperature superconductivity in iron-based materials. *Nature Physics.* **6** (9), 645 (2010).
2. Keimer, B., Kivelson, S. A., Norman, M. R., Uchida, S., Zaanen, J. From quantum matter to high-temperature superconductivity in copper oxides. *Nature.* **518**, 179-186 (2015).
3. Anderson, P. W. Physics: The opening to complexity. *Proceedings of the National Academy of Sciences of the United States of America.* **92** (15), 6653-6654 (1995).
4. Dagotto, E. Complexity in strongly correlated electronic systems. *Science*. **309**, 257-262 (2005).
5. Davis, J. S., Lee, D.-H. Concepts relating magnetic interactions, intertwined electronic orders, and strongly correlated superconductivity. *Proceedings of the National Academy of Sciences of the United States of America.* **110** (44), 17623-17630 (2013).
6. Fernandes, R., Chubukov, A., Schmalian, J. What drives nematic order in iron-based superconductors? *Nature Physics.* **10** (2), 97 (2014).
7. Fradkin, E., Kivelson, S. A., Tranquada, J. M. Colloquium: Theory of intertwined orders in high temperature superconductors. *Reviews of Modern Physics.* **87** (2), 457 (2015).
8. Stillwell, E., Skove, M., Davis, J. Two “Whisker” Straining Devices Suitable for Low Temperatures. *Review of Scientific Instruments.* **39** (2), 155-157 (1968).
9. Shayegan, M. et al. Low-temperature, in situ tunable, uniaxial stress measurements in semiconductors using a piezoelectric actuator. *Applied Physics Letters.* **83** (25), 5235-5237 (2003).
10. Chu, J.-H., Kuo, H.-H., Analytis, J. G., Fisher, I. R. Divergent nematic susceptibility in an iron arsenide superconductor. *Science.* **337** (6095), 710-712 (2012).
11. Song, Y. et al. Uniaxial pressure effect on structural and magnetic phase transitions in NaFeAs and its comparison with as-grown and annealed BaFe2As2. *Physical Review B.* **87** (18), 184511 (2013).
12. Allan, M. P. et al. Anisotropic impurity states, quasiparticle scattering and nematic transport in underdoped Ca(Fe1−xCox)2As2. *Nature Physics.* **9** (4), 220-224 (2013).
13. Hicks, C. W. et al. Strong increase of Tc of Sr2RuO4 under both tensile and compressive strain. *Science.* **344** (6181), 283-285 (2014).
14. Hicks, C. W., Barber, M. E., Edkins, S. D., Brodsky, D. O., Mackenzie, A. P. Piezoelectric-based apparatus for strain tuning. *Review of Scientific Instruments.* **85** (6), 065003 (2014).
15. Gannon, L. et al. A device for the application of uniaxial strain to single crystal samples for use in synchrotron radiation experiments. *Review of Scientific Instruments.* **86** (10), 103904 (2015).
16. Kretzschmar, F. et al. Critical spin fluctuations and the origin of nematic order in Ba(Fe1−xCox)2As 2. *Nature Physics.* **12** (6), 560 (2016).
17. Steppke, A. et al. Strong peak in T c of Sr2RuO4 under uniaxial pressure. *Science.* **355** (6321), 133 (2017).
18. Yim, C. M. et al. Discovery of a strain-stabilised smectic electronic order in LiFeAs. *Nature Communications.* **9** (1), 2602 (2018).
19. Gao, S. et al. Atomic-scale strain manipulation of a charge density wave. *Proceedings of the National Academy of Sciences of the United States of America.* **115** (27), 6986-6990 (2018).
20. Jiang, J. et al. Distinct in-plane resistivity anisotropy in a detwinned FeTe single crystal: Evidence for a Hund's metal. *Physical Review B.* **88** (11), 115130 (2013).

21. Zhang, Y. et al. Symmetry breaking via orbital-dependent reconstruction of electronic structure in detwinned NaFeAs. *Physical Review B.* **85** (8), 085121 (2012).
22. Watson, M. D., Haghighirad, A. A., Rhodes, L. C., Hoesch, M., Kim, T. K. Electronic anisotropies revealed by detwinned angle-resolved photo-emission spectroscopy measurements of FeSe. *New Journal of Physics.* **19** (10), 103021 (2017).
23. Iida, K. et al. Strong T c dependence for strained epitaxial Ba(Fe1-xCox)2As2 thin films. *Applied Physics Letters.* **95** (19), 192501 (2009).
24. Stern, A., Dzero, M., Galitski, V., Fisk, Z., Xia, J. Surface-dominated conduction up to 240 K in the Kondo insulator SmB 6 under strain. *Nature Materials.* **16** (7), 708-711 (2017).
25. Iida, K. et al. Hall-plot of the phase diagram for Ba(Fe1−xCox)2As2. *Scientific Reports.* **6**, 28390 (2016).
26. Hänke, T. et al. Reorientation of the diagonal double-stripe spin structure at Fe1+yTe bulk and thin-film surfaces. *Nature Communications.* **8**, 13939 (2017).
27. Takeshita, N., Sasagawa, T., Sugioka, T., Tokura, Y., Takagi, H. J. Gigantic anisotropic uniaxial pressure effect on superconductivity within the CuO2 plane of La1.64Eu0.2Sr0.16CuO4: Strain control of stripe criticality. *Journal of the Physical Society of Japan.* **73** (5), 1123-1126 (2004).
28. Kuo, H.-H., Shapiro, M. C., Riggs, S. C., Fisher, I. R. Measurement of the elastoresistivity coefficients of the underdoped iron arsenide Ba(Fe0.975Co0.025)2As2. *Physical Review B.* **88** (8), 085113 (2013).
29. He, M. et al. Dichotomy between in-plane magnetic susceptibility and resistivity anisotropies in extremely strained BaFe2As2. *Nature Communications.* **8** (1), 504 (2017).
30. Engelmann, J. et al. Strain induced superconductivity in the parent compound BaFe2As2. *Nature Communications.* **4** (2877), 2877 (2013).
31. Böhmer, A. et al. Effect of biaxial strain on the phase transitions of Ca(Fe1−xCox)2As2. *Physical Review Letters.* **118** (10), 107002 (2017).
32. Bao, W. et al. Tunable (δ π, δ π)-type antiferromagnetic order in α-Fe(Te,Se) superconductors. *Physical Review Letters.* **102** (24), 247001 (2009).
33. Koz, C., Rößler, S., Tsirlin, A. A., Wirth, S., Schwarz, U. Low-temperature phase diagram of Fe1+yTe studied using x-ray diffraction. *Physical Review B.* **88** (9), 094509 (2013).
34. Enayat, M. et al. Real-space imaging of the atomic-scale magnetic structure of Fe1+yTe. *Science.* **345** (6197), 653-656 (2014).
35. Singh, U. R., Aluru, R., Liu, Y., Lin, C., Wahl, P. Preparation of magnetic tips for spin-polarized scanning tunneling microscopy on Fe1+yTe. *Physical Review B.* **91** (16), 161111 (2015).
36. Chandra, S., Islam, A. K. M. A. Elastic and electronic properties of PbO-type FeSe1-xTex (x= 0-1.0): A first-principles study. *ArXiv preprint.* arXiv:1008**.1448** (2010).

Figure 1

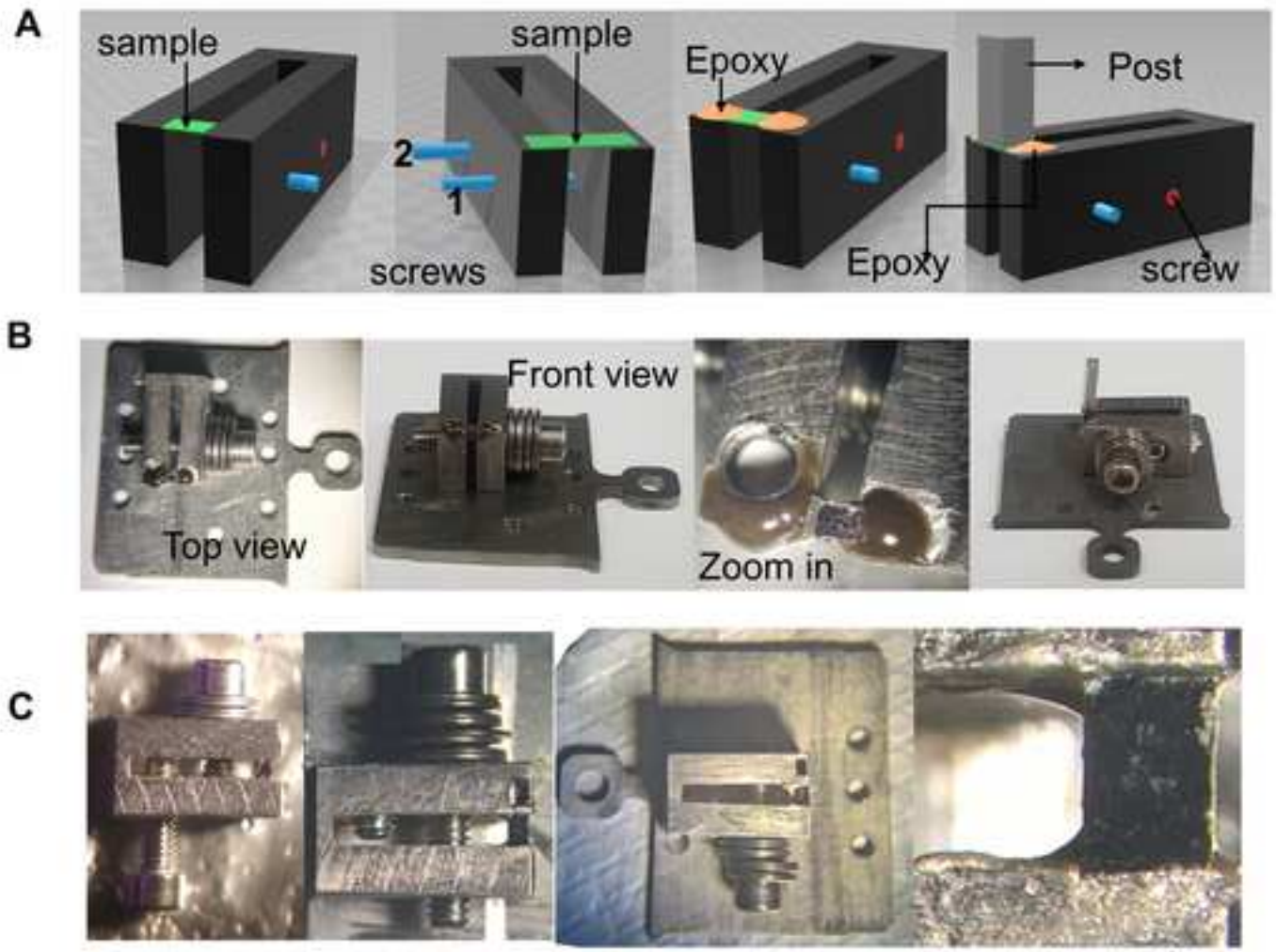

Figure 2

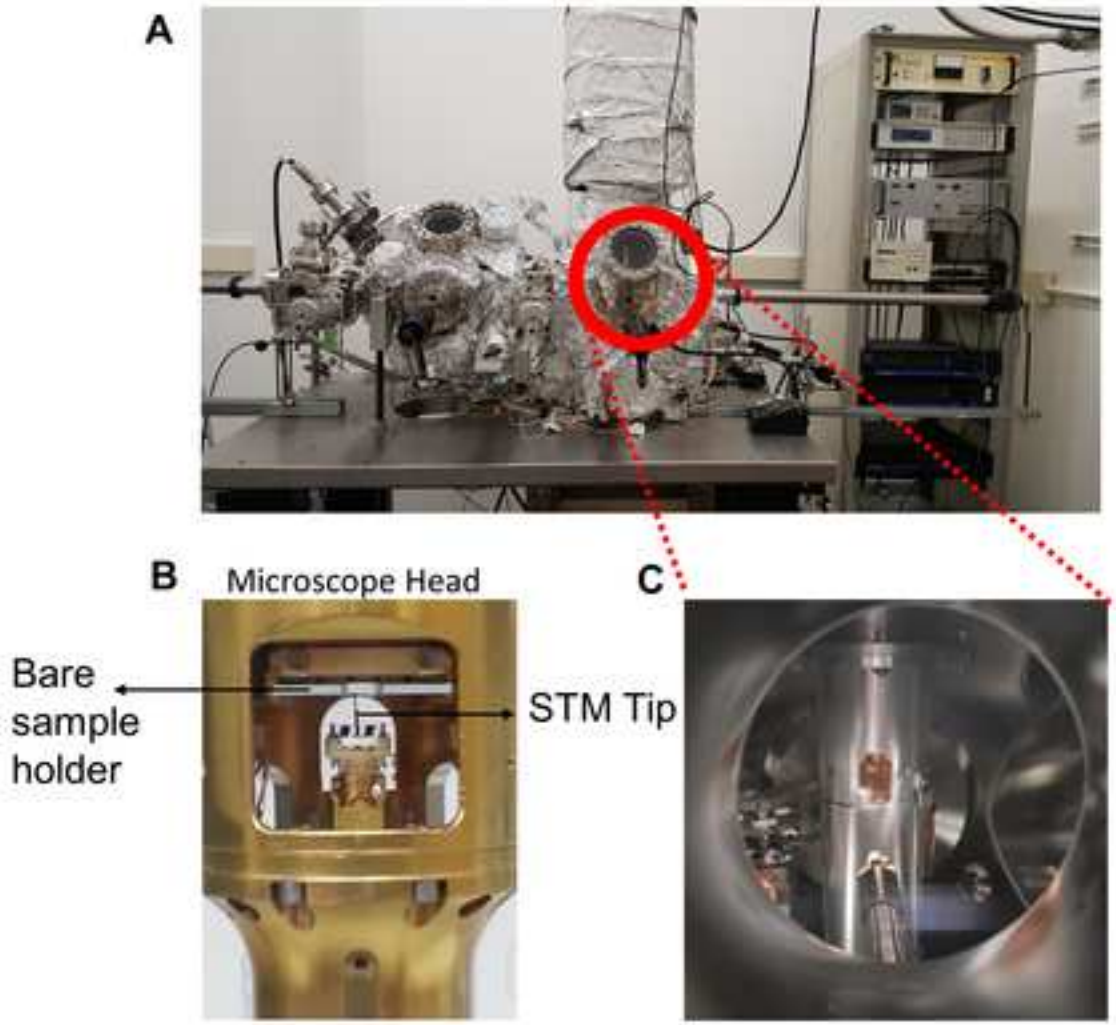

Figure 3

Click here to access/download;Figure;Figure_3.png

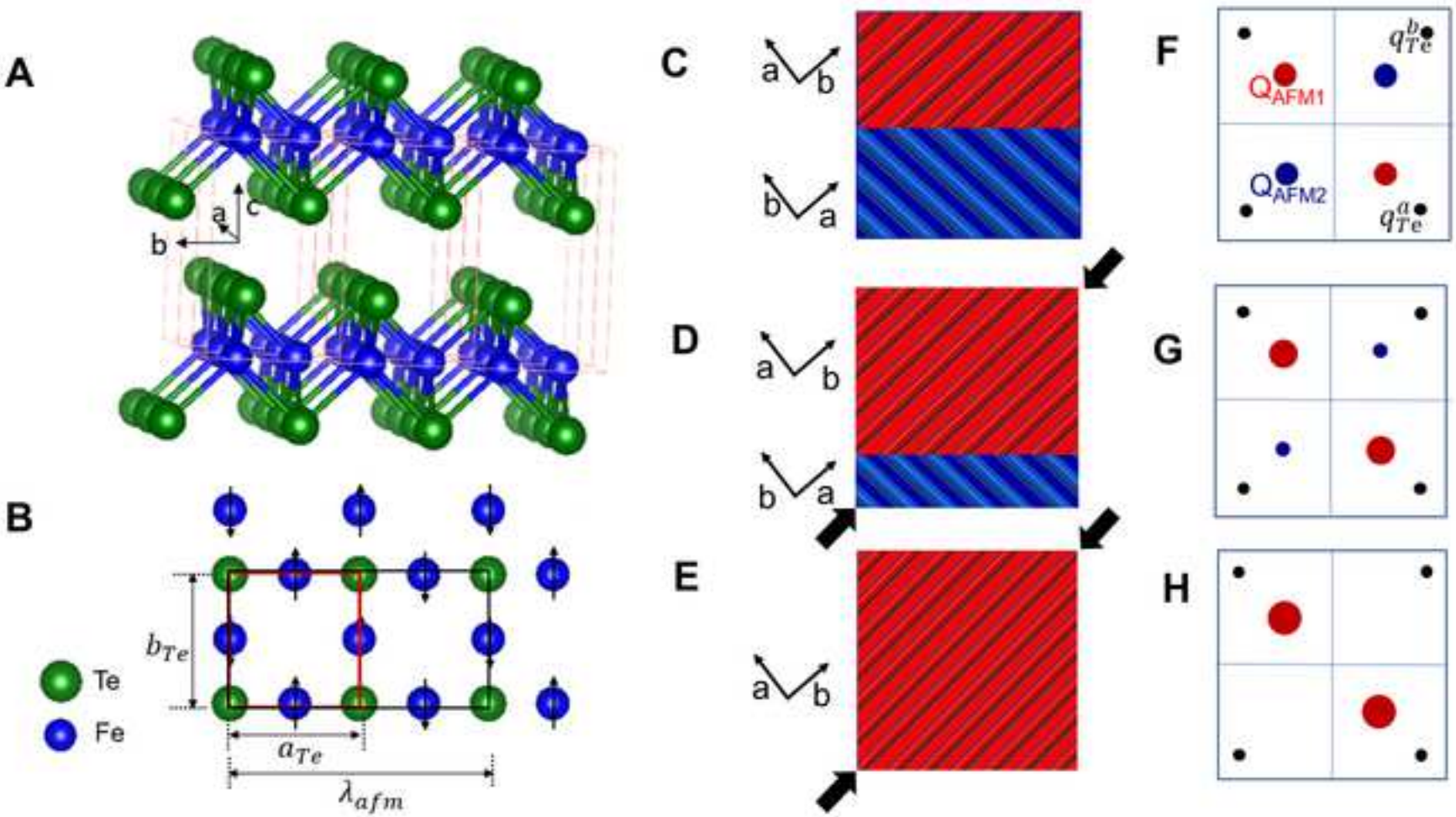

Figure 4

Click here to access/download;Figure;Figure_4.png

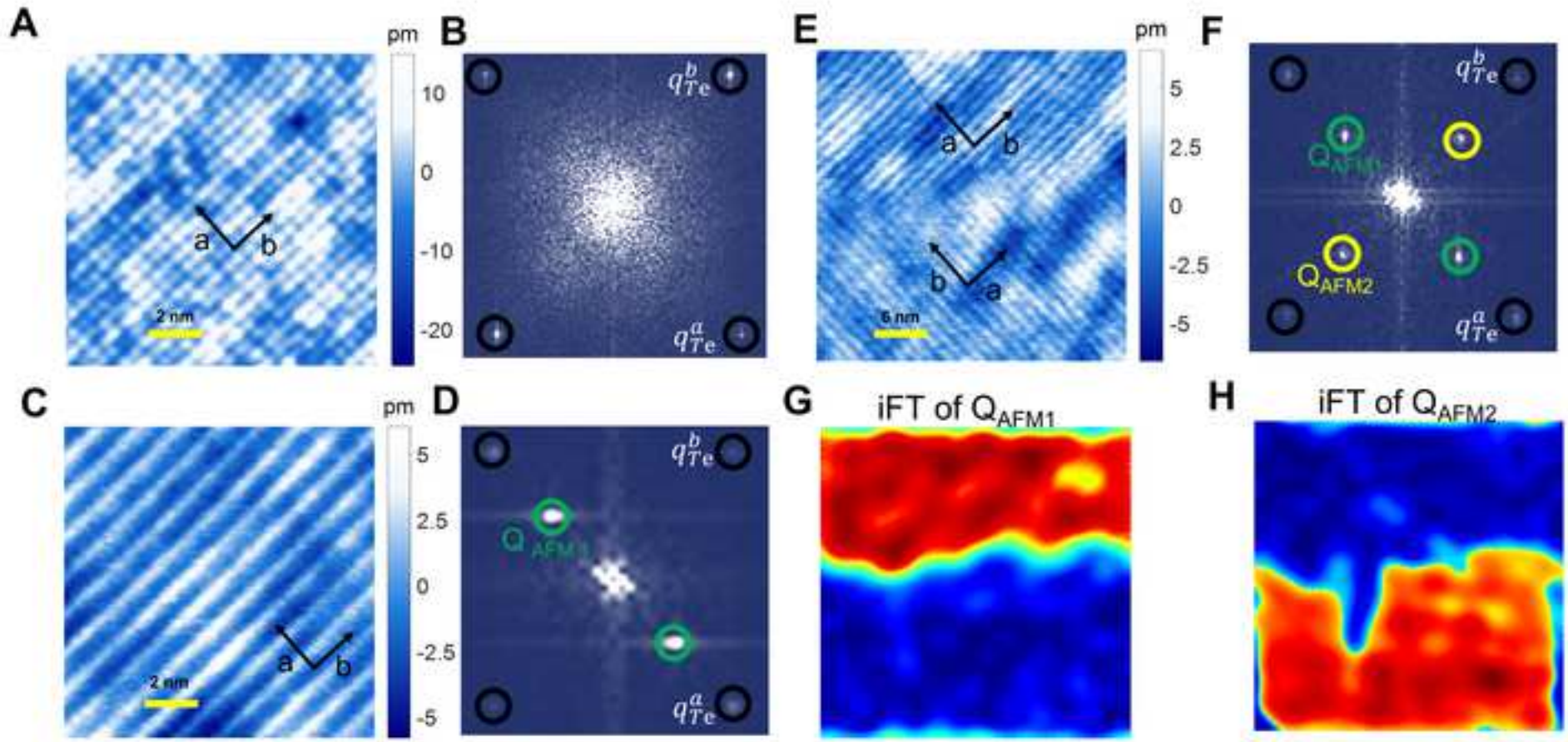

Figure 5

Click here to access/download;Figure;Figure_5.png

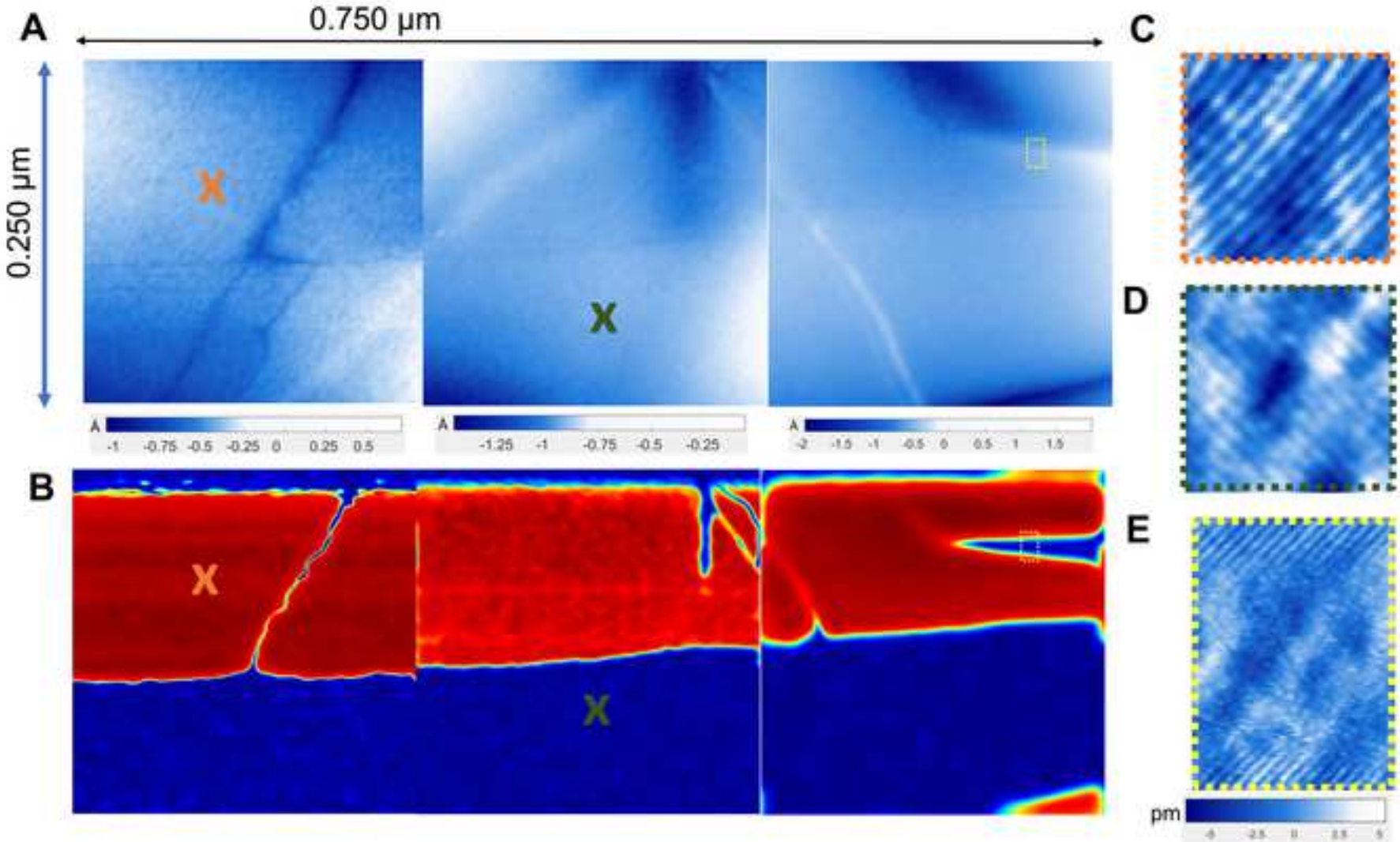

Figure 6

Click here to access/download;Figure;Figure_6.png

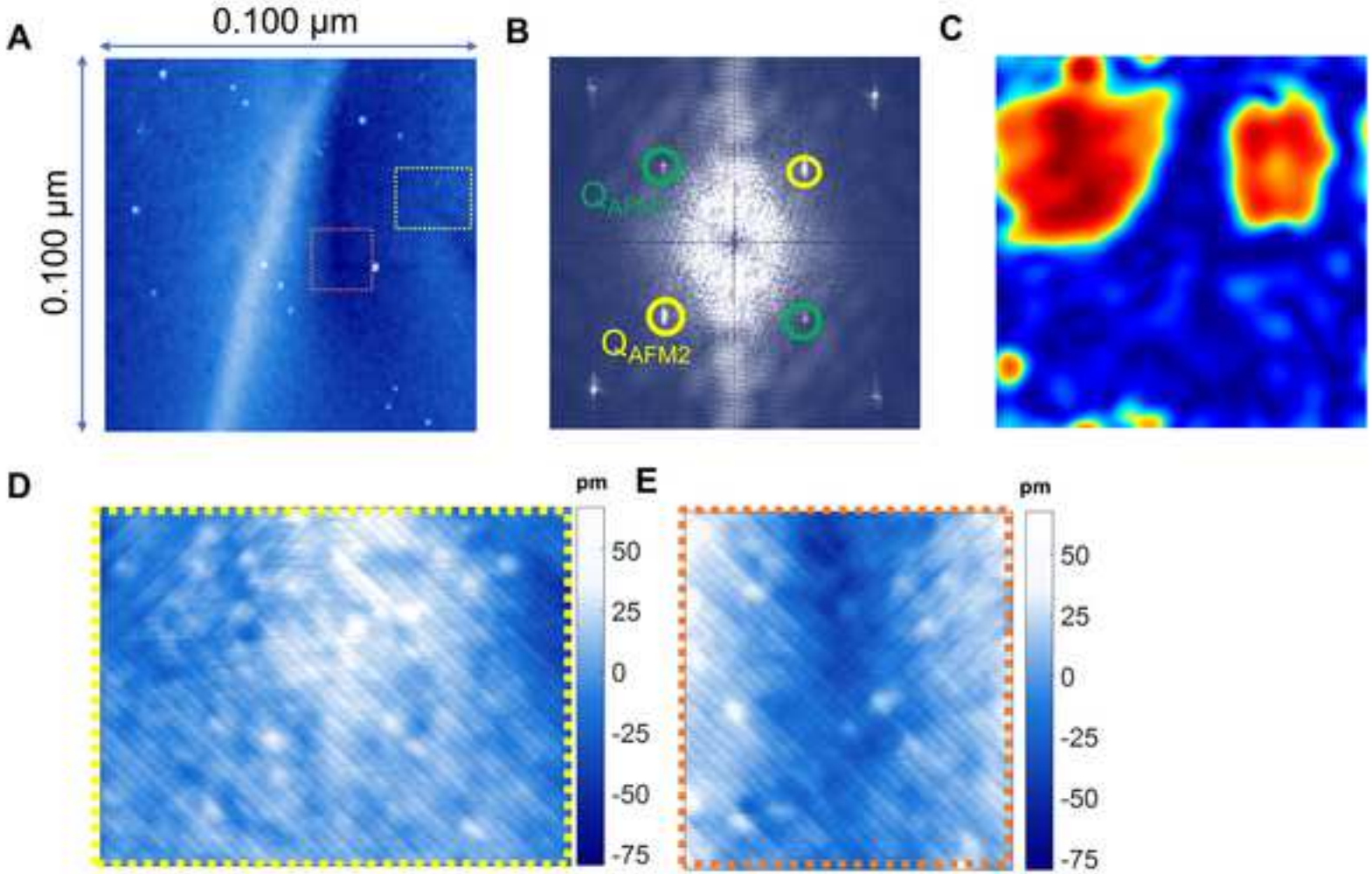

Figure 7

Click here to access/download;Figure;Figure_7.png

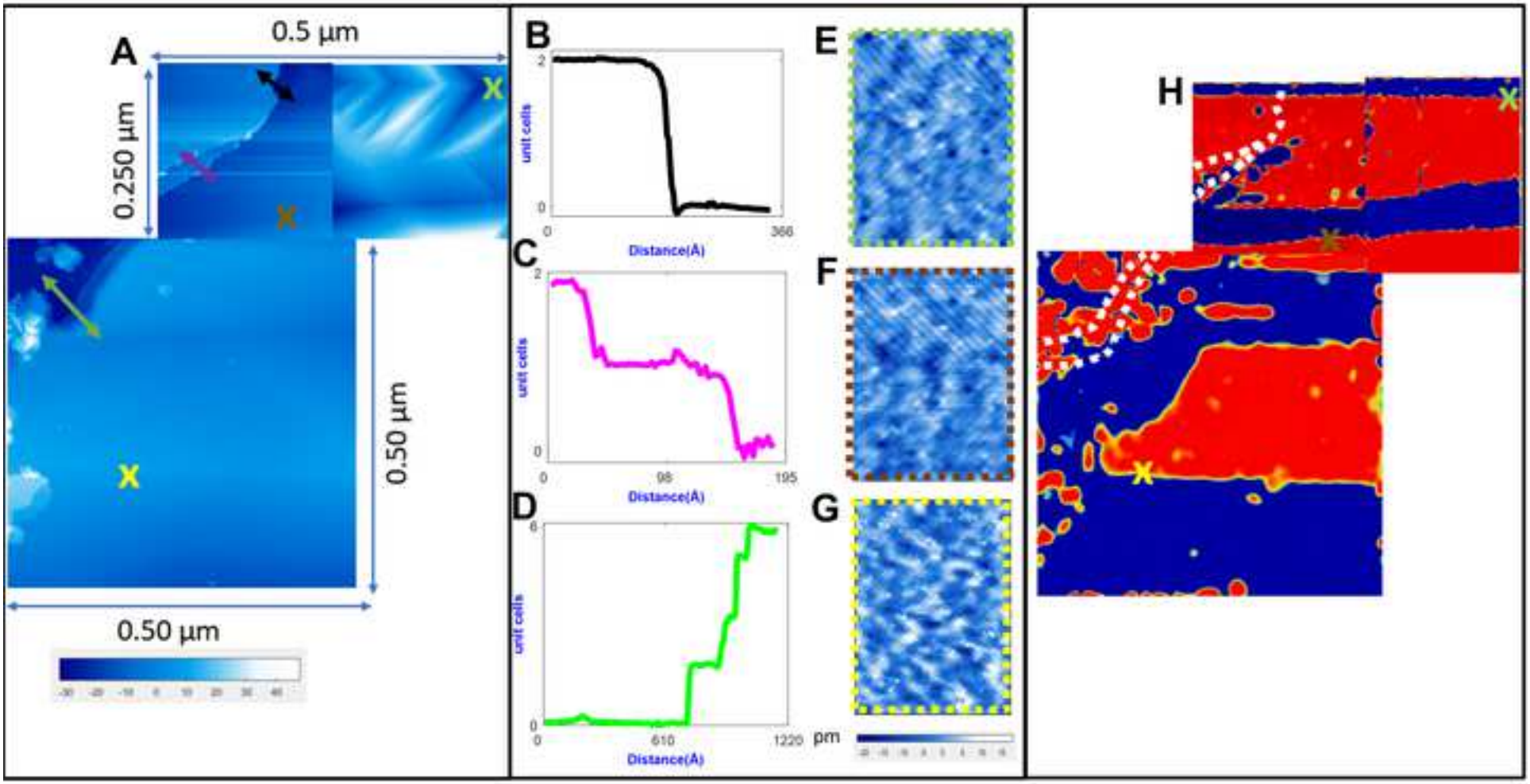

Figure 8

Click here to access/download;Figure;Figure_8.png

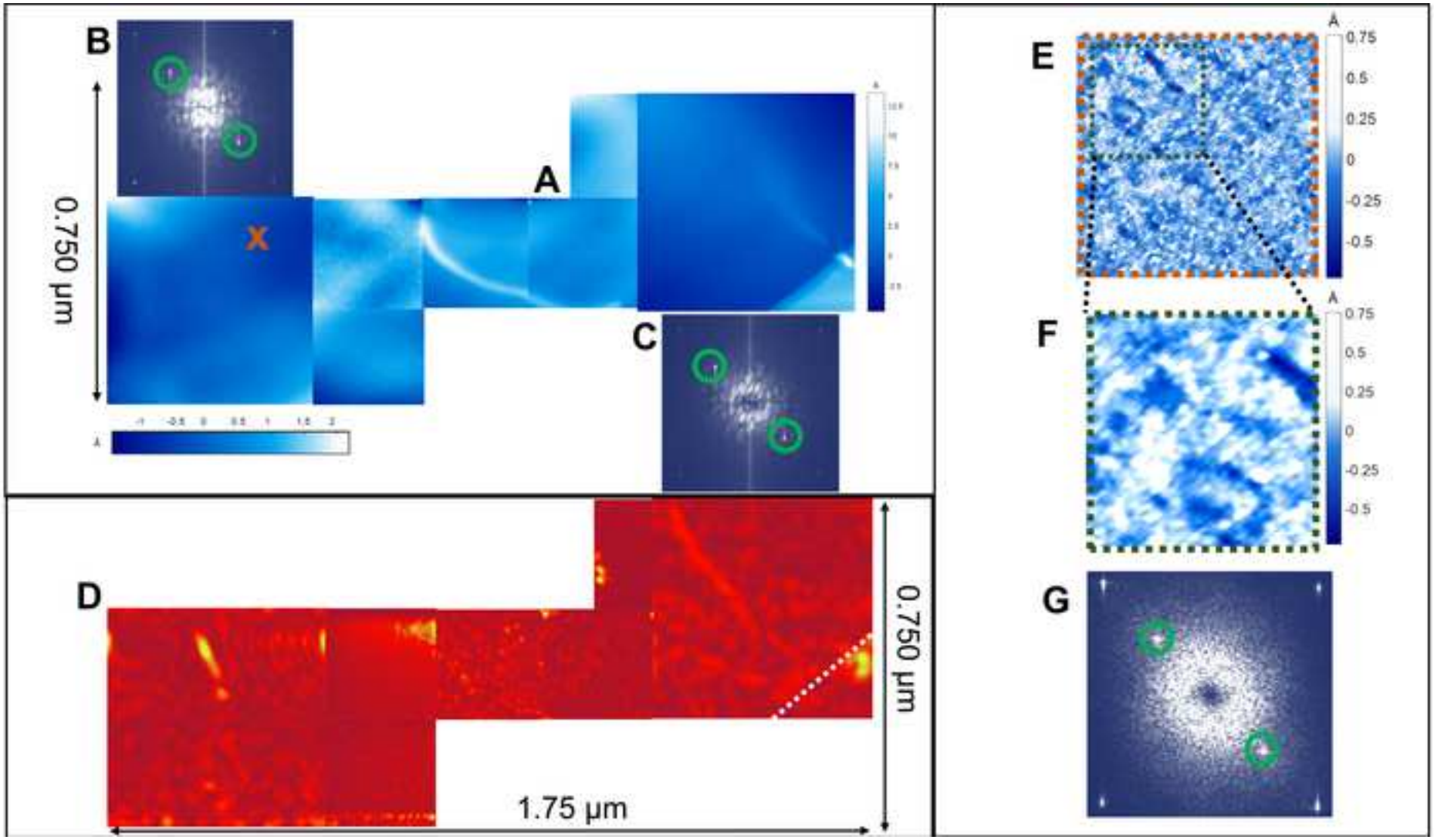

Name of Material/ Equipment	Company	Catalog Number	Comments/Description
Belleville spring disks	McMaster Carr		
Fe(1.1)Te			Single Crystal
H20E	Epoxy Technology		
H74F	Epoxy Technology		
Micrometer screws	McMaster Carr		
Stainless Steel sheets (416)	McMaster Carr		

jove JOURNAL OF VISUALIZED EXPERIMENTS
1 Alewife Center #200
Cambridge, MA 02140
tel. 617.945.9051
www.jove.com

ARTICLE AND VIDEO LICENSE AGREEMENT

Title of Article: Visualizing uniaxial-strain-manipulation of antiferomagnetic domains in FeTe using spin polarized scanning tunneling microscope

Author(s): M. Kavai, I. Giannakis, J. Leshen, J. Friedman, P. Zajdel, P. Aynajian

Item 1: The Author elects to have the Materials be made available (as described at http://www.jove.com/publish) via:

☒ Standard Access ☐ Open Access

Item 2: Please select one of the following items:

☒ The Author is **NOT** a United States government employee.

☐ The Author is a United States government employee and the Materials were prepared in the course of his or her duties as a United States government employee.

☐ The Author is a United States government employee but the Materials were NOT prepared in the course of his or her duties as a United States government employee.

ARTICLE AND VIDEO LICENSE AGREEMENT

1. **Defined Terms.** As used in this Article and Video License Agreement, the following terms shall have the following meanings: "**Agreement**" means this Article and Video License Agreement; "**Article**" means the article specified on the last page of this Agreement, including any associated materials such as texts, figures, tables, artwork, abstracts, or summaries contained therein; "**Author**" means the author who is a signatory to this Agreement; "**Collective Work**" means a work, such as a periodical issue, anthology or encyclopedia, in which the Materials in their entirety in unmodified form, along with a number of other contributions, constituting separate and independent works in themselves, are assembled into a collective whole; "**CRC License**" means the Creative Commons Attribution-Non Commercial-No Derivs 3.0 Unported Agreement, the terms and conditions of which can be found at: http://creativecommons.org/licenses/by-nc-nd/3.0/legalcode; "**Derivative Work**" means a work based upon the Materials or upon the Materials and other pre-existing works, such as a translation, musical arrangement, dramatization, fictionalization, motion picture version, sound recording, art reproduction, abridgment, condensation, or any other form in which the Materials may be recast, transformed, or adapted; "**Institution**" means the institution, listed on the last page of this Agreement, by which the Author was employed at the time of the creation of the Materials; "**JoVE**" means MyJove Corporation, a Massachusetts corporation and the publisher of The Journal of Visualized Experiments; "**Materials**" means the Article and / or the Video; "**Parties**" means the Author and JoVE; "**Video**" means any video(s) made by the Author, alone or in conjunction with any other parties, or by JoVE or its affiliates or agents, individually or in collaboration with the Author or any other parties, incorporating all or any portion of the Article, and in which the Author may or may not appear.

2. **Background.** The Author, who is the author of the Article, in order to ensure the dissemination and protection of the Article, desires to have the JoVE publish the Article and create and transmit videos based on the Article. In furtherance of such goals, the Parties desire to memorialize in this Agreement the respective rights of each Party in and to the Article and the Video.

3. **Grant of Rights in Article.** In consideration of JoVE agreeing to publish the Article, the Author hereby grants to JoVE, subject to **Sections 4** and **7** below, the exclusive, royalty-free, perpetual (for the full term of copyright in the Article, including any extensions thereto) license (a) to publish, reproduce, distribute, display and store the Article in all forms, formats and media whether now known or hereafter developed (including without limitation in print, digital and electronic form) throughout the world, (b) to translate the Article into other languages, create adaptations, summaries or extracts of the Article or other Derivative Works (including, without limitation, the Video) or Collective Works based on all or any portion of the Article and exercise all of the rights set forth in (a) above in such translations, adaptations, summaries, extracts, Derivative Works or Collective Works and(c) to license others to do any or all of the above. The foregoing rights may be exercised in all media and formats, whether now known or hereafter devised, and include the right to make such modifications as are technically necessary to exercise the rights in other media and formats. If the "Open Access" box has been checked in **Item 1** above, JoVE and the Author hereby grant to the public all such rights in the Article as provided in, but subject to all limitations and requirements set forth in, the CRC License.

4. **Retention of Rights in Article.** Notwithstanding the exclusive license granted to JoVE in **Section 3** above, the Author shall, with respect to the Article, retain the non-exclusive right to use all or part of the Article for the non-commercial purpose of giving lectures, presentations or teaching classes, and to post a copy of the Article on the Institution's website or the Author's personal website, in each case provided that a link to the Article on the JoVE website is provided and notice of JoVE's copyright in the Article is included. All non-copyright intellectual property rights in and to the Article, such as patent rights, shall remain with the Author.

5. **Grant of Rights in Video – Standard Access.** This **Section 5** applies if the "Standard Access" box has been checked in **Item 1** above or if no box has been checked in **Item 1** above. In consideration of JoVE agreeing to produce, display or otherwise assist with the Video, the Author hereby acknowledges and agrees that, Subject to **Section 7** below, JoVE is and shall be the sole and exclusive owner of all rights of any nature, including, without limitation, all copyrights, in and to the Video. To the extent that, by law, the Author is deemed, now or at any time in the future, to have any rights of any nature in or to the Video, the Author hereby disclaims all such rights and transfers all such rights to JoVE.

6. **Grant of Rights in Video – Open Access.** This **Section 6** applies only if the "Open Access" box has been checked in **Item 1** above. In consideration of JoVE agreeing to produce, display or otherwise assist with the Video, the Author hereby grants to JoVE, subject to **Section 7** below, the exclusive, royalty-free, perpetual (for the full term of copyright in the Article, including any extensions thereto) license (a) to publish, reproduce, distribute, display and store the Video in all forms, formats and media whether now known or hereafter developed (including without limitation in print, digital and electronic form) throughout the world, (b) to translate the Video into other languages, create adaptations, summaries or extracts of the Video or other Derivative Works or Collective Works based on all or any portion of the Video and exercise all of the rights set forth in (a) above in such translations, adaptations, summaries, extracts, Derivative Works or Collective Works and (c) to license others to do any or all of the above. The foregoing rights may be exercised in all media and formats, whether now known or hereafter devised, and include the right to make such modifications as are technically necessary to exercise the rights in other media and formats. For any Video to which this **Section 6** is applicable, JoVE and the Author hereby grant to the public all such rights in the Video as provided in, but subject to all limitations and requirements set forth in, the CRC License.

7. **Government Employees.** If the Author is a United States government employee and the Article was prepared in the course of his or her duties as a United States government employee, as indicated in **Item 2** above, and any of the licenses or grants granted by the Author hereunder exceed the scope of the 17 U.S.C. 403, then the rights granted hereunder shall be limited to the maximum rights permitted under such statute. In such case, all provisions contained herein that are not in conflict with such statute shall remain in full force and effect, and all provisions contained herein that do so conflict shall be deemed to be amended so as to provide to JoVE the maximum rights permissible within such statute.

8. **Protection of the Work.** The Author(s) authorize JoVE to take steps in the Author(s) name and on their behalf if JoVE believes some third party could be infringing or might infringe the copyright of either the Author's Article and/or Video.

9. **Likeness, Privacy, Personality.** The Author hereby grants JoVE the right to use the Author's name, voice, likeness, picture, photograph, image, biography and performance in any way, commercial or otherwise, in connection with the Materials and the sale, promotion and distribution thereof. The Author hereby waives any and all rights he or she may have, relating to his or her appearance in the Video or otherwise relating to the Materials, under all applicable privacy, likeness, personality or similar laws.

10. **Author Warranties.** The Author represents and warrants that the Article is original, that it has not been published, that the copyright interest is owned by the Author (or, if more than one author is listed at the beginning of this Agreement, by such authors collectively) and has not been assigned, licensed, or otherwise transferred to any other party. The Author represents and warrants that the author(s) listed at the top of this Agreement are the only authors of the Materials. If more than one author is listed at the top of this Agreement and if any such author has not entered into a separate Article and Video License Agreement with JoVE relating to the Materials, the Author represents and warrants that the Author has been authorized by each of the other such authors to execute this Agreement on his or her behalf and to bind him or her with respect to the terms of this Agreement as if each of them had been a party hereto as an Author. The Author warrants that the use, reproduction, distribution, public or private performance or display, and/or modification of all or any portion of the Materials does not and will not violate, infringe and/or misappropriate the patent, trademark, intellectual property or other rights of any third party. The Author represents and warrants that it has and will continue to comply with all government, institutional and other regulations, including, without limitation all institutional, laboratory, hospital, ethical, human and animal treatment, privacy, and all other rules, regulations, laws, procedures or guidelines, applicable to the Materials, and that all research involving human and animal subjects has been approved by the Author's relevant institutional review board.

11. **JoVE Discretion.** If the Author requests the assistance of JoVE in producing the Video in the Author's facility, the Author shall ensure that the presence of JoVE employees, agents or independent contractors is in accordance with the relevant regulations of the Author's institution. If more than one author is listed at the beginning of this Agreement, JoVE may, in its sole

discretion, elect not take any action with respect to the Article until such time as it has received complete, executed Article and Video License Agreements from each such author. JoVE reserves the right, in its absolute and sole discretion and without giving any reason therefore, to accept or decline any work submitted to JoVE. JoVE and its employees, agents and independent contractors shall have full, unfettered access to the facilities of the Author or of the Author's institution as necessary to make the Video, whether actually published or not. JoVE has sole discretion as to the method of making and publishing the Materials, including, without limitation, to all decisions regarding editing, lighting, filming, timing of publication, if any, length, quality, content and the like.

12. **Indemnification.** The Author agrees to indemnify JoVE and/or its successors and assigns from and against any and all claims, costs, and expenses, including attorney's fees, arising out of any breach of any warranty or other representations contained herein. The Author further agrees to indemnify and hold harmless JoVE from and against any and all claims, costs, and expenses, including attorney's fees, resulting from the breach by the Author of any representation or warranty contained herein or from allegations or instances of violation of intellectual property rights, damage to the Author's or the Author's institution's facilities, fraud, libel, defamation, research, equipment, experiments, property damage, personal injury, violations of institutional, laboratory, hospital, ethical, human and animal treatment, privacy or other rules, regulations, laws, procedures or guidelines, liabilities and other losses or damages related in any way to the submission of work to JoVE, making of videos by JoVE, or publication in JoVE or elsewhere by JoVE. The Author shall be responsible for, and shall hold JoVE harmless from, damages caused by lack of sterilization, lack of cleanliness or by contamination due to the making of a video by JoVE its employees, agents or independent contractors. All sterilization, cleanliness or decontamination procedures shall be solely the responsibility of the Author and shall be undertaken at the Author's expense. All indemnifications provided herein shall include JoVE's attorney's fees and costs related to said losses or damages. Such indemnification and holding harmless shall include such losses or damages incurred by, or in connection with, acts or omissions of JoVE, its employees, agents or independent contractors.

13. **Fees.** To cover the cost incurred for publication, JoVE must receive payment before production and publication of the Materials. Payment is due in 21 days of invoice. Should the Materials not be published due to an editorial or production decision, these funds will be returned to the Author. Withdrawal by the Author of any submitted Materials after final peer review approval will result in a US$1,200 fee to cover pre-production expenses incurred by JoVE. If payment is not received by the completion of filming, production and publication of the Materials will be suspended until payment is received.

14. **Transfer, Governing Law.** This Agreement may be assigned by JoVE and shall inure to the benefits of any of JoVE's successors and assignees. This Agreement shall be governed and construed by the internal laws of the Commonwealth of Massachusetts without giving effect to any conflict of law provision thereunder. This Agreement may be executed in counterparts, each of which shall be deemed an original, but all of which together shall be deemed to me one and the same agreement. A signed copy of this Agreement delivered by facsimile, e-mail or other means of electronic transmission shall be deemed to have the same legal effect as delivery of an original signed copy of this Agreement.

A signed copy of this document must be sent with all new submissions. Only one Agreement is required per submission.

CORRESPONDING AUTHOR

Name:	Pegor Aynajian
Department:	Physics, Applied Physics, and Astronomy
Institution:	Binghamton University
Title:	Assistant Professor
Signature:	
Date:	10/4/2018

Please submit a **signed** and **dated** copy of this license by one of the following three methods:

1. Upload an electronic version on the JoVE submission site
2. Fax the document to +1.866.381.2236
3. Mail the document to JoVE / Attn: JoVE Editorial / 1 Alewife Center #200 / Cambridge, MA 02140

We thank the reviewers for their time and efforts. Below we provide further clarification of the remarks raised by the reviewers

Reviewer #1 (Remarks to the Author):

Manuscript Summary:
The manuscript reports on a uniaxial strain device integrated to the STM instrument. The effect of the uniaxial strain is clearly observed. And the protocol and uniaxial strain devices are clearly discussed.

Minor Concerns:
The manuscript is lacking a description how they make the tip spin-polarized. Is there something special about how they interact the tip with the Fe surface to pick up those atoms for SP-STM? The layout of figures 7,8 is difficult to follow. Maybe clear boundaries around the collated figures could help the reader.

To achieve spin-polarized STM, the last atoms of the STM tip has to be coated with magnetic atoms, which can be quite challenging. In this case of studying Fe1+yTe, the sample itself provides a simple means of achieving this. The excess irons (y concentration in Fe1+yTe) are weakly bound on the cleaved surface. Scanning the tip at low bias and with high enough current exceeding a few nA brings the tip in close proximity to these Fe atoms and a few of those atoms can be picked up by the tip. Successful preparation of a spin polarized tip is revealed by the magnetic contrast in the topography whose periodicity is twice that of the lattice constant of top tellurium atoms. This additional modulation is the antiferromagnetic order in the sample.

We have added a section on how we made our tip spin polarized. We have also made changes on figure 7 and 8 that could help the reader, as suggested by the referee.

Reviewer #2 (Remarks to the Author):

Manuscript Summary:
The authors present a uniaxial strain device which can be used in ultra-high vacuum for surface sensitive measurements such as STM and ARPES. The device turns out to be very efficient to obtain a single AFM domain in FeTe. It is very important to study the intrinsic physical properties in materials which suffer from the twin structures and i recommend the publication of this paper after considering the following concerns i have:

Major Concerns:

(1) As mentioned, the device can be used for applying both compressive and tensile strain, however, the authors only show one set of strained data in Fig.8. The authors should specify what kind of strain they applied on this data. And it will be better that the authors can show data with both strain added.

We thank the referee for this important question. In our experiments a compressive strain was applied by rotating the micrometer screw by 50 degrees. The applied pressure is transmitted through the springs and correspond to a uniaxial pressure of 0.08 GPa. From the in-plain Young's modulus of FeTe of 70GPa, the applied uniaxial pressure can be converted to 0.1% uniaxial strain. In the new manuscript we have clarified the applied compressive strain magnitude.

The device is designed so that in an analogous way a tensile strain can be applied, yet the latter has not been tested so far. In the manuscript we emphasized that while both compressive and tensile strain applications are analogous in nature, tensile strain has not been tested yet.

(2) To have an idea of how uniform the strain is by using this device, i would suggest the author to include a figure showing the AFM domain at different sample positions (As the sample should be around 1mm*2mm size, it will be better the authors can show the region around the corner, in the center, etc.)

This is also very important question. We mention in the manuscript that STM is done near the center of the sample where the strain is expected to be maximum (see ref.14 of the main manuscript for a theoretical model). We have studied the variation of the strain on various locations, and as long as the tip is within a few hundred microns of the center of the sample no domains are found, indicating a rather uniform strain. However, when we move the STM tip to edge of the sample, domains do appear. This is expected since the edges of the sample, which are epoxied on top of the device will not experience strain. This has been clarified in the new manuscript.

Minor Concerns:

There are already some studies reported before using the similar design to do the transport measurement (Phys. Rev. B 88, 115130 (2013)) and ARPES measurement (Phy. Rev. B 85, 085121 (2012), New J. Phys. 19 103021 (2017)) which cleaved the single crystal in situ with the strain applied. The authors should cite them.

Thank you for providing this information, the citations have been added to the new manuscript.

Reviewer #3 (Remarks to the Author):

Manuscript Summary:
This manuscript report a new experimental protocol for providing tunable strains to the samples investigated by scanning tunneling microscopy.
Such protocols are important in condensed matter physics and very few publications outline details in the experimental protocol of applying strain.
In this context the manuscript is quite relevant for a broad audience of experimentalists. The authors also demonstrate their technique using parent compound of
iron based superconductors (Fe(1+g)Te).The manuscript is written in a clear way outlining all relevant details.

Minor Concerns:
The only possibly concern related to this work is a question of how easy/or difficult is to apply this experimental protocol on other classes of materials.

This is a fair question and bit tricky to answer. One of the major difficulties is the cleaving process itself. For layered systems which are easily cleaved the success rate is high. We have successfully applied this technique to Bi2212, high temperature superconductor, in both STM and resonant x-ray studies. However, when dealing with samples that lack a natural cleavage plane, one may face new challenges.

We thank the editors for their time and efforts. We have clarified all the information that has been requested of us.

Editorial comments

1. After revision, please upload a .doc/.docx version of your revised manuscript to your Editorial Manager account (this may be why you had problems uploading your previous revisions).
2. 1.3: What is the sample here, and how exactly is it cut?

The sample is Fe1.1Te single crystal, we have added that information to the text and details on how it is cut.

3. 2.2: How is the device baked?

The device is baked in a convection oven, we have included this information in the text.

4. 2.4: Around how much should the screw be turned here? You mention 50 degrees later, but can this be modified?

Yes, it can be modified, and we have added that information in the text.

5. 3/4: Please provide more detail here-how exactly is the STM controlled? If by software, please provide specific steps (e.g, “click”, “open”, etc.).

We have added information on the R9 software that controls the STM, and a link to RHK Technology, which are the manufacturers of the STM for more detailed information. Unfortunately, this is a complicated software that the user must be very familiar with, in order to carry out any experiment.

6. Figure 1A: In the legend, by (A, C) and (A,B), do you mean the figure panels? It’s unclear.

Yes, we mean the figure panels. I have clarified that in the text to make it easier to follow.